

Nondestructive Characterization of Materials Using Laser-Generated Ultrasound

Sang-Woo Choi and Joon-Hyun Lee*
*School of Mechanical Engineering
Pusan National University, Pusan 609-735, Korea*

Abstract. It is recently well recognized that the technique for the one-sided stress wave velocity measurement in structural materials provides valuable information on the state of the material such as quality, uniformity, location of cracked or damaged area. This technique is especially effective to measure velocities of longitudinal and Rayleigh waves when access to only one surface of structure is possible. However, one of problems for one-sided stress wave velocity measurement is to get consistent and reliable source for the generation of elastic wave. In this study, the laser based surface elastic wave was used to provide consistent and reliable source for the generation of elastic wave into the materials. The velocities of creeping wave and Rayleigh wave in materials were measured by the one-sided technique using laser based surface elastic wave. These wave velocities were compared with bulk wave velocities such as longitudinal wave and shear wave velocities to certify accuracy of measurement. In addition, the mechanical properties such as poisson's ratio and specific modulus(E/ρ) were calculated with the velocities of surface elastic waves.

Key Words : *Laser-generated Ultrasound, Wave Velocity, Elastic Modulus, One-sided Technique*

1. INTRODUCTION

The degradation of materials by corrosion and chemical reactions produces variation of the material properties. Since there is a relation between material properties and the velocities of elastic waves, materials can be evaluated nondestructively by measuring the velocities of elastic waves. The one-sided technique provides reasonable measurements of the velocities of elastic waves when it is impossible to apply the pulse/echo or through-transmission methods because of high attenuation of the ultrasonic waves in the material or when the surface, except for one side, is intricate.

* Corresponding Author
E-mail address: johlee@pusan.ac.kr

In the conventional one-sided technique, elastic waves are generated by dropping a steel ball from a certain position onto the surface of the specimen. It is difficult to obtain precise results with the steel ball drop method since the source of the elastic waves, the impact, is not consistent. Therefore, a DC powered solenoid with a spring-loaded steel shaft was used for impact consistency. Time domain signals captured from each receiver usually contain high levels of incoherent noises which obscure the signal of the creeping wave. In order to reduce this noise level, the computer program summed numerous signals resulting from repeated impacts. However, it takes too much time to manually select the received signals, due to problems such as the electric noise caused by solenoid switching and missing triggering time remaining. In this study, the one-sided technique was improved by using a pulse laser as the impact source. Capturing the elastic waves was automated by using the Q-switch trigger of the pulse laser to reduce the time of signal processing. The intensity of the impact, which is the source of the elastic waves, was controlled by adjusting the energy of the pulse laser.

In this study, the one-side technique and the laser-based ultrasonic technique were combined to nondestructively evaluate the material properties by measuring the elastic waves on the surface. The elastic waves were generated with a Nd:YAG (Neodymium-Doped Yttrium-Aluminum-Garnet) pulse laser on steel, and cemented carbide alloy, which are metallic materials or mortar, which a nonmetallic material. The velocities of the surface elastic waves were measured from the elastic waves received on a surface where the pulse laser was illuminated. Material properties, such as Poisson's ratio(ν) and specific elastic modulus(E/ρ), were calculated and velocities were verified by comparing them with elastic wave velocities determined from conventional ultrasonic testing.

2. LASER-BASED ULTRASONIC AND ONE-SIDED TECHNIQUES

The one-sided technique was developed to measure the creeping wave and the Rayleigh wave velocities at the same time, with two receivers placed on the same surface to nondestructively evaluate semi-infinite media such as concrete, pavement and other materials. The one-sided technique is useful to measure elastic properties and to evaluate damage when there is only one accessible surface. In addition, when the conventional ultrasonic testing is not available, the one-sided technique makes it possible to measure the velocity of elastic waves in thick materials, because of the high attenuation in wave propagation. The one-sided technique was firstly applied to measure longitudinal wave velocities in concrete by Long et al (1945). In the mid 1950s, Whitehurst (1954) used a hammer to generate transient elastic waves, which propagate on the surface of concrete. Signals of these transient elastic waves were obtained by two accelerometers on the surface. The arrival time for each accelerometer was measured by measuring the time of the first disturbance signal. In the most previous studies, elastic properties were calculated based on an assumed Poisson's ratio value for the concrete. The surface wave velocity between two receiving sensors was obtained from the cross-correlation data compiled by Wu et al. (1995). The obtained velocity data agrees with the surface wave velocity measured using the through-transmission method in ultrasonic testing, when receiving sensors were located farther than 15cm from the source of impact. Qixian et al. (1996)

proposed measuring the longitudinal wave and the Rayleigh wave velocities simultaneously by generating elastic waves with an ultrasonic wave transducer. Popovics et al. (1998) and Lee et al. (1999) measured the longitudinal wave velocity and the Rayleigh wave velocity simultaneously using the one-sided technique. In that technique, the striker, driven by a DC powered solenoid, was used for generating the elastic waves. However, the generated elastic waves were not consistent. Furthermore, the elastic constants could not be evaluated exactly, because the longitudinal and shear wave velocities are required for calculating elastic moduli in these previous works, the measured velocities of the elastic waves were not based on shear wave velocities, but on Rayleigh wave velocities.

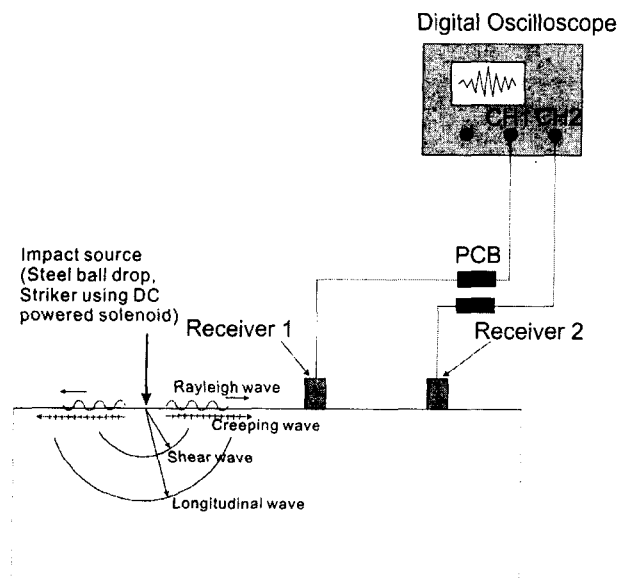


Fig. 1. Schematic diagram of the generation and reception of the transient wave using one-sided technique.

The principle of the one-sided technique is described in Fig. 1. Transient elastic waves are generated from the impact source by dropping a steel ball or striker driven by a DC powered solenoid. There are various modes of elastic waves generated in the material and its surface, such as longitudinal wave, shear wave, creeping wave, and Rayleigh wave. The creeping wave is the longitudinal mode wave on the surface and the Rayleigh wave is the shear vertical mode wave on the surface. The creeping wave and Rayleigh wave are simultaneously obtained by two PZT on the surface. The velocities of these waves are calculated from the distance between the two sensors and time delay of each wave arrival. In this paper, a combination of the one-sided technique and the laser-generated ultrasonic technique is proposed for estimating material properties based on the consistent elastic waves generated. In order to calculate the elastic moduli, the shear wave velocity was calculated from the creeping wave velocity and the Rayleigh wave velocity was deduced by numerical approximation.

3. MEASUREMENT OF MATERIAL PROPERTIES FROM ELASTIC WAVES

The nondestructive evaluation technique using laser-based surface elastic waves is shown in Fig. 2. Surface elastic waves, which were generated with a laser, were received using two piezoelectric accelerometer sensors located along a line on the surface of the test specimen. The diameter of the accelerometer was 5.6mm and the resonance frequency was 80kHz. The distance from the impact source to the nearest accelerometer (IP) was 50mm, and the spacing between the two accelerometers (X) was 30mm. A shock excitation of thermal expansion was applied by the pulse illumination of a Q-switched pulse laser at a point on the surface of the specimen. The first accelerometer sensor, which was the nearest receiver to the elastic wave source, received the surface elastic waveform after it had propagated as long as IP from the wave generation source. The second accelerometer sensor received the surface elastic waveform after it had propagated as long as X from the first sensor. The acquisition of these waveforms was synchronized with pulse laser illumination by using Q-switch triggering.

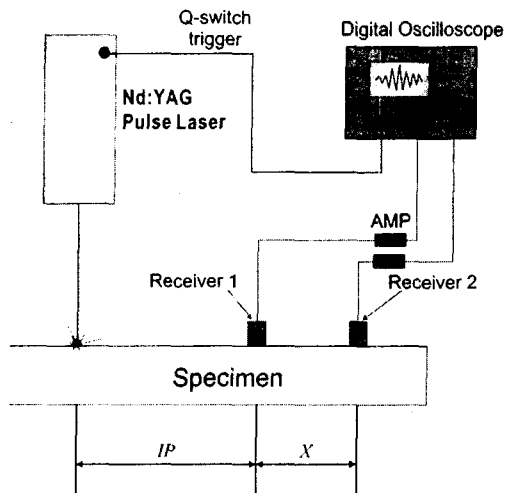


Fig. 2. Schematic diagram of experimental set-up.

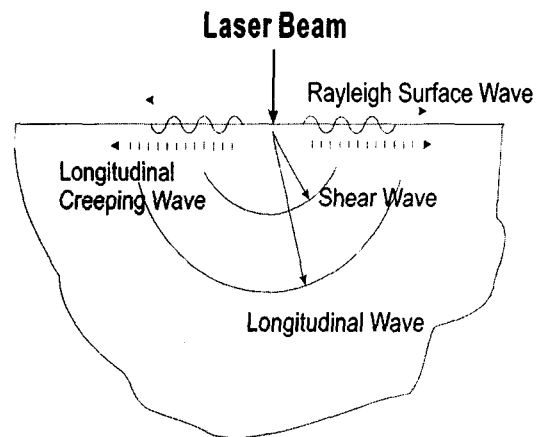


Fig. 3. Generated elastic waves with pulse laser.

The longitudinal wave and the shear wave (spherical wave modes) were propagated in bulk and the creeping wave and the Rayleigh wave (surface wave modes) were propagated on the surface by the generation of elastic waves with a pulse laser, as shown in Fig. 3. Elastic waves on the surface were captured with accelerometers mounted on the surface. Displacement of particles due to the creeping wave is parallel to the direction of wave propagation on the surface, and the displacement of particles due to the Rayleigh wave is perpendicular to the direction of wave propagation on the surface. Accelerometers are sensitive to motion that is perpendicular to the surface. Therefore, the Rayleigh wave was dominant in the waveforms, which were acquired with the accelerometers. However, it was not easy to distinguish the creeping wave from the waveforms because of the low amplitude of the creeping wave compared with the noise signals. These elastic wave

signals were stored after being amplified and digitalized with a digital oscilloscope (LeCroy 9310A). Since the arrival signal of creeping wave can be obscured by incoherent noise signals, the noise signals were reduced by averaging 100 repeated signals. This time-averaging was conducted with a synchronizing Q-switch trigger signal.

The waveforms of the elastic waves, which were generated with the pulse laser, are shown in Fig. 4. The arrival time of the creeping wave was determined where flight time was $16 \mu\text{s}$ after Q-switch triggering. The Rayleigh wave arrived later, since the velocity of the creeping wave is the same as that of the longitudinal wave, and the velocity of the Rayleigh wave is similar to that of the shear wave. The first positive peak of the Rayleigh wave was determined as the arrival time of the Rayleigh wave, as shown in Fig. 4.

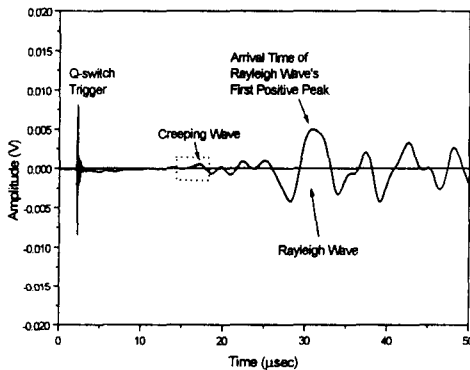


Fig. 4. Typical signal and arrival time of waves.

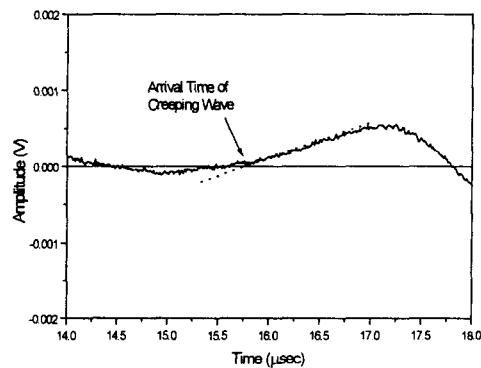


Fig. 5. Arrival time of creeping wave.

The arrival time of the creeping wave was determined as the intersection of the zero level and the first increasing slope of the creeping wave, as shown in Fig. 5. The flight time (Δt) for the creeping wave and the Rayleigh wave between the two accelerometers was measured using the arrival times of the two waveforms, which were acquired with each accelerometer.

The velocities of the creeping wave and the Rayleigh wave velocities were calculated using X , the distance between the two accelerometers, and the flight times, as shown by Eq. (1).

$$C = \frac{X}{\Delta t} \quad (1)$$

The material properties, such as modulus of elasticity (E), shear modulus of elasticity (G), density (ρ) and Poisson's ratio (ν), are related to the velocities of the longitudinal wave, the shear wave and the Rayleigh wave, as shown in Eqs. (2) and (4).

$$C_l = \sqrt{\frac{E(1-\nu)}{\rho(1+\nu)(1-2\nu)}} \quad (2)$$

$$C_s = \sqrt{\frac{G}{\rho}} = \sqrt{\frac{E}{2(1+\nu)\rho}} \quad (3)$$

$$C_r = \frac{0.87 + 1.12\nu}{1 + \nu} C_s \quad (4)$$

The Poisson's ratio and elastic modulus over density are represented by Eq. (5) and Eq. (6), which result from Eq. (2) and Eq. (3). Therefore, the Poisson's ratio and the specific modulus were calculated from the velocities measured by Eq. (1).

$$\nu = \frac{2C_s^2 - C_l^2}{2C_s^2 - 2C_l^2} \quad (5)$$

$$\frac{E}{\rho} = \frac{(1+\nu)(1-2\nu)}{(1-\nu)} C_l^2 = \left(\frac{4C_s^2 - 3C_l^2}{C_s^2 - C_l^2} \right) C_s^2 \quad (6)$$

Since the velocity of the shear wave was unknown, the velocity was calculated using Eq. (4) and Eq. (5) and numerical iteration of these, as shown in Fig. 6. In the first step, a temporary Poisson's ratio was calculated using Eq. (5), where C_l is the velocity of the creeping wave and C_s is the velocity of the shear wave. Since the shear wave velocity was unknown and Rayleigh wave velocity is generally about 90% of the shear wave velocity, the Rayleigh wave velocity can be used initially instead of the shear wave velocity in Eq. (5) in the iterating calculation procedure. In the next step, the temporary velocity of the shear wave was calculated using Eq. (4), where ν is the temporary Poisson's ratio, which was calculated in the previous step, and C_r is the velocity of the measured Rayleigh wave. With this temporary velocity calculation of the shear wave, a more precise Poisson's ratio was calculated using Eq. (5). After repeating these sequences, the velocity of the shear wave and Poisson's ratio approached exact values. After calculating Poisson's ratio and the velocity of the shear wave, elastic modulus over density (E/ρ) was calculated using Eq. (6), where C_l is the velocity of the creeping wave.

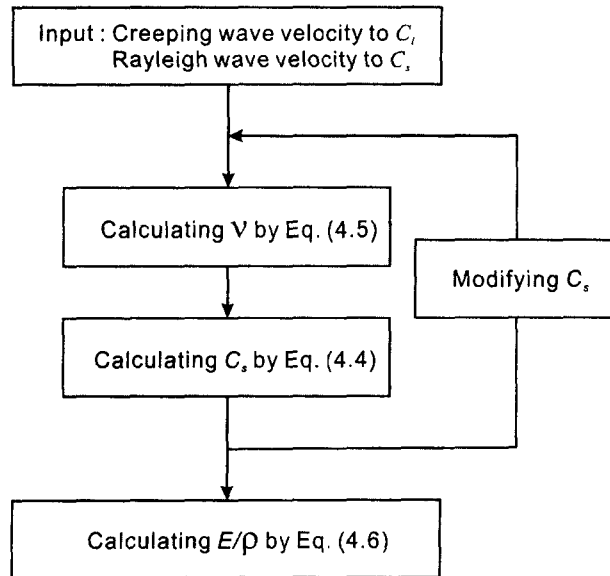


Fig. 6. Flowchart of iteration for obtaining v , C_s , E/ρ .

4. EXPERIMENTAL RESULTS AND DISCUSSION

The collection of data for the evaluation of the material properties of steel (SM400) was conducted by receiving surface elastic waves generated by a pulse laser. The dimensions of the thick steel plate were $300\text{mm} \times 300\text{mm} \times 48.9\text{mm}$. Two sensors acquired the elastic surface waveform on the steel surface, as shown in Fig. 7, after each illumination of the pulse laser on the same surface. There were noise signals, which were generated by the Q-switch trigger, where flight time was $5 \mu\text{s}$. The components of the creeping waves and the Rayleigh waves were contained in the waveforms acquired by both sensors. Since the velocity of the creeping waves is about twice the velocity of the Rayleigh waves, the arrival time of the creeping waves is approximately half of the arrival time of the Rayleigh waves after the noise signal of the Q-switch trigger. The first sensor ($R1$) recorded the arrival of the creeping waves at $t=13 \mu\text{s}$ and the second sensor ($R2$) recorded the arrival of the creeping waves at $t=19 \mu\text{s}$. The first positive peak of the Rayleigh waves arrived at $t=23 \mu\text{s}$ for the first sensor ($R1$), and at $t=34 \mu\text{s}$ for second sensor ($R2$).

A Fast Fourier Transform (FFT) spectrum of a waveform received on the surface of the steel by the first sensor was analyzed for frequency characteristics, as shown in Fig. 8. There were two high peaks in frequency domain. The frequency of first peak was 79 kHz , which was almost equal to the resonance frequency (80 kHz) of the receiving sensor. The frequency of the other peak was 397 kHz , which was five times the resonance frequency of the receiving sensor, which was the dominant frequency component of the waveform.

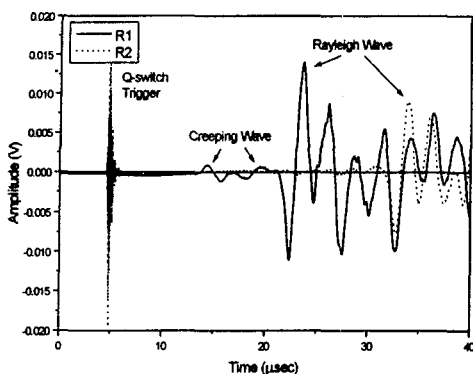


Fig. 7. Experimental waveform. (Steel)

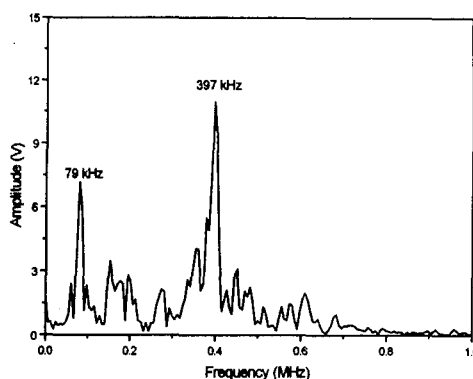


Fig. 8. FFT spectrum. (Steel, R1)

The elastic surface wave velocities were calculated and measured using both the one-sided technique with laser-generated elastic waves and a conventional ultrasonic testing technique employing the pulse-echo method, as shown in Table 1. This was done in order to compare the results of using surface waves with the results of using bulk waves. A longitudinal wave transducer of 5 MHz and a shear wave transducer of 5 MHz were used to measure the velocities of elastic wave propagation with the conventional ultrasonic testing technique. From the measured velocities of elastic waves, shear wave velocities and material properties, such as Poisson's ratio (ν) and specific elastic modulus (E/ρ), were calculated, using Eqs. (4), (5) and (6), respectively. The difference between the velocity of the creeping waves measured using the one-sided technique and the velocity of the longitudinal waves measured using a conventional ultrasonic technique, was 0.5%. This is in accordance with the idea that the velocity of creeping waves is the same as the velocity of longitudinal waves. The velocity of the Rayleigh waves was 90.7% of the velocity of the shear waves which were measured using the conventional ultrasonic testing technique. The velocity of shear waves, calculated with Eq. (4) and Eq. (5), differed by as much as 2% from the velocity of the shear waves measured using a conventional ultrasonic testing

Table 1. Elastic wave velocities and material properties of steel

Measured Value	Surface wave velocity	Creeping wave	5,953 m/s
		Rayleigh wave	2,944 m/s
	Bulk wave velocity	Longitudinal wave	5,920 m/s
		Shear wave	3,247 m/s
Calculated Value	Poisson's ratio		0.3006
	Shear wave velocity		3,178 m/s
	E/ρ		$2.6281 \times 10^7 \text{ m}^2/\text{s}^2$

technique.

4.2 Surface Elastic Waves on Cemented Carbide Alloy

The properties of cemented carbide alloy were evaluated using surface elastic waves generated by a pulse laser, and were compared with the results for steel. The dimensions of the cemented carbide alloy were 150mm×150mm×9.85mm. The two waveforms of elastic surface waves generated by the laser pulses are shown in Fig. 9. There was a high frequency fluctuation on the low frequency signal.

The dominant frequencies, 79 kHz, 153 kHz and 397 kHz, were the FFT spectrum of waveforms received by the first sensor on the surface of the cemented carbide alloy, as shown in Fig. 10. A difference between the frequency characteristics of steel and cemented carbide alloy is that the magnitude at 397 kHz was high for steel, but low for cemented carbide alloy, while the magnitude at 79 kHz was high for cemented carbide alloy, but low for steel. In addition, the magnitude at 153 kHz, which was twice of resonance frequency of the receiving sensor, rose for cemented carbide alloy. The high frequency fluctuation in Fig. 8 was the component of 397 kHz, and the low frequency trend was the component of 79 kHz.

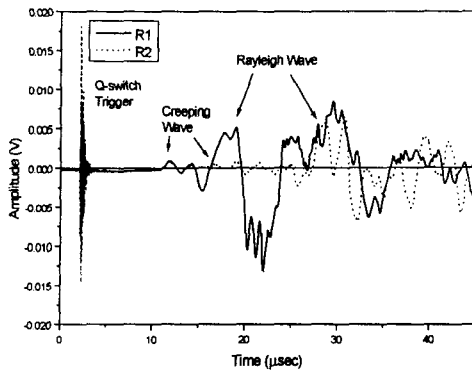


Fig. 9. Experimental waveform. (Cemented carbide alloy)

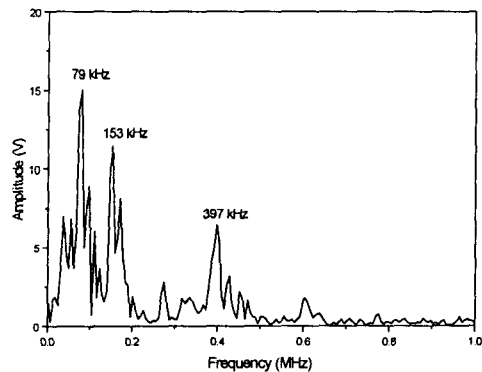


Fig. 10. FFT spectrum. (Cemented carbide alloy, R1)

Creeping wave and Rayleigh wave velocities based on were measured for cemented carbide alloy using the one-sided technique and laser-based surface elastic waves. While, longitudinal and shear wave velocities were measured, in bulk, using the pulse echo method, as shown in Table 2. In addition, shear wave velocities and material properties, such as Poisson's ratio and specific elastic modulus, were calculated from the measured velocities of elastic surface waves. The velocity of the creeping waves that propagated on the surface was 6,085 m/s, and the velocity of the bulk longitudinal waves was 6,090 m/s. The difference between the two velocities was not more than 0.1%. This shows that the velocity of the longitudinal waves could be measured precisely by measuring the velocity of the creeping waves. The velocity of the shear wave, which was calculated based on the velocities of the surface waves, was 3,409 m/s, and the measured velocity of the bulk shear waves was 3,267 m/s. The difference between the velocities of the shear waves was

4%, which was caused by the velocity of the Rayleigh waves, and was not precisely measured due to the imprecise measurement of the arrival times of the Rayleigh waves. This imprecise data was due to the superposition of high frequency and low frequency components. The measured velocity of the Rayleigh waves was less precise than the measured velocity of the creeping waves. The velocities of longitudinal waves and shear waves in cemented carbide alloy were higher than the velocities in steel. As expected, the calculated specific modulus of elasticity for cemented carbide alloy was higher than the specific modulus of elasticity for steel. The calculated Poisson's ratio was higher for steel than for cemented carbide alloy.

Table 2. Elastic wave velocities and material properties of cemented carbide alloy

Measured Value	Surface wave velocity	Creeping wave	6,085 m/s
		Rayleigh wave	3,141 m/s
	Bulk wave velocity	Longitudinal wave	6,090 m/s
		Shear wave	3,267 m/s
Calculated Value	Poisson's ratio		0.2712
	Shear wave velocity		3,409 m/s
	E/ρ		$2.9554 \times 10^7 \text{ m}^2/\text{s}^2$

4.3 Surface Elastic Waves on Mortar

Elastic surface waves on mortar, generated with the illumination of a pulse laser, were obtained using two accelerometers, as shown in Fig. 11. The low amplitude of the elastic waves was due to attenuation in the propagation of the waves. It is too difficult to measure ultrasonic wave velocities in bulk because of the high attenuation, even when using low frequency ultrasonic waves in thick mortar. However, using the one-side technique in concert with laser-generated elastic surface waves provides feasible measurements of wave propagating velocities. This method is not dependent on the thickness of materials, and surface waves have lower attenuation than bulk waves.

A peak of 159 kHz in the frequency domain had the highest magnitude in the frequency spectrum, as shown in Fig. 12. The magnitude of peaks, such as 40 kHz, 80 kHz, 120 kHz and 160 kHz, became higher as frequency increased. However, attenuation caused by scattering resulted in a decrease in magnitude for frequency bands higher than 200 kHz.

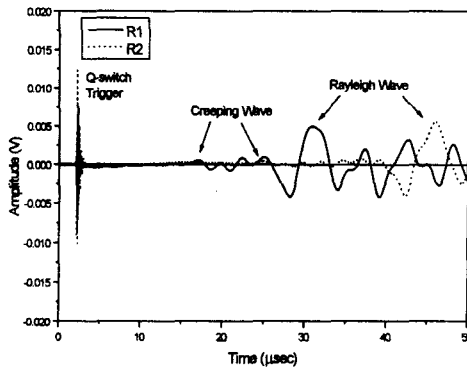


Fig. 11. Experimental waveform. (Mortar)

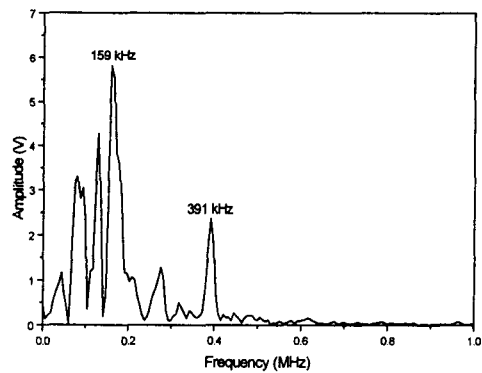


Fig. 12. FFT spectrum. (Mortar, R1)

The velocity of surface elastic waves was measured and the velocity of shear waves and material properties, such as Poisson's ratio and specific elastic modulus, were calculated from the measured surface elastic wave velocities, as shown in Table 3. The velocity of the creeping waves was 3,861 m/s and the velocity of the Rayleigh waves was 2,012 m/s. Elastic waves in mortar are slower than in steel or in cemented carbide alloy. The specific elastic modulus for mortar, which was calculated from the measured surface elastic wave velocities, was less than half that of the specific elastic modulus for steel or cemented carbide alloy.

Table 3. Elastic wave velocities and material properties of mortar

Measured Value	Surface wave velocity	Creeping wave	3,861 m/s
		Rayleigh wave	2,012 m/s
Calculated Value	Poisson's ratio		0.2638
	Shear wave velocity		2,187 m/s
	E/ρ		$1.2089 \times 10^7 \text{ m}^2/\text{s}^2$

It was possible to measure the velocity of bulk elastic waves using the pulse-echo method for both steel and cemented carbide alloy. However, the attenuation in mortar made it impossible to measure the velocity of elastic waves using a 5 MHz ultrasonic transducer and the conventional ultrasonic technique. The one-sided technique, using laser-based surface elastic waves, made it possible to measure the velocity of elastic waves in mortar, which could not be accurately measured using the conventional technique.

5. CONCLUSIONS

For the purpose of enhancing the consistency of the generation of elastic waves in the one-sided technique, the source of the surface elastic wave generation was the illumination of a pulse laser, as opposed to dropping a steel ball or striking a hammer on the material. Therefore, the longitudinal wave and shear wave velocities were measured using the one-sided technique with automated signal acquisition.

From the results of measuring the ultrasonic velocities for steel and cemented carbide alloy, it was shown that precise longitudinal wave velocities were obtained by measuring the creeping wave velocity with the one-sided technique, using laser-generated elastic waves. Because the Rayleigh wave velocity data was imprecise due to the interaction of various frequency components, there were errors in the shear wave velocity data obtained using the one-sided technique. The elastic wave velocities for mortar can not be measured using the conventional ultrasonic testing technique because of the ultrasonic wave attenuation that occurs for frequency bands higher than 200 kHz. However, the longitudinal wave and the shear wave velocities for mortar could be obtained based on the creeping wave and the Rayleigh wave velocity measurements obtained by using the one-sided technique with laser-generated surface elastic waves.

This one-sided technique using laser-generated elastic waves is promising in regard to the measurement of elastic wave velocities and material properties in cases where the conventional ultrasonic testing technique can not be applied because of attenuation in the elastic wave propagation or the limitation of accessible surface.

ACKNOWLEDGEMENTS

This study was supported by Korea Institute of Science & Technology Evaluation and Planning (KISTEP) and Ministry of Science & Technology (MOST), Korean government, through its Basic Atomic Energy Research Institute (BAERI) Program.

REFERENCES

- Long, B. G., Kurtz, H. J. and Sandenaw, T. A. (1945). An Instrument and a Technique for Field Determination of Modulus of Elasticity and Flexural Strength of Concrete Pavements, *Journal of the American Concrete Institute*, **16**, 217-231.
- Whitehurst, E. A. (1954). Pulse-Velocity Techniques and Equipment for Testing Concrete, *Proceeding of the Highway Research Board*, **33**, 226-242.
- Wu, T. T., Fang, J. S., Liu, G. Y. and Kuo, M. K. (1995). Determination of Elastic Constants of a Concrete Specimen Using Transient Waves, *Journal of the Acoustical Society of America*, **98**, 2142-2148.

- Qixian, L., and Bungey, J. H. (1996). Using Compression Wave Ultrasonic Transducers to Measure the Velocity of Surface Waves and Hence Determine Dynamic Modulus of Elasticity for Concrete, *Construction and Building Materials*, **10**, 237-242.
- Popovics, J. S., Lee, J. H., Song, W. J. and Achenbach, J. D. (1998). One-sided Stress Wave Measurement in Concrete, *J. of Eng. Mechanics*, **124**, 12, 1346-1353.
- Lee, J. H., Park, W. S., Popovics, J. S. and Achenbach, J. D.(1999). Application of One-Sided Stress Wave Velocity Measurement Technique to Evaluate Freeze-Thaw Damage in Concrete, *Review of Progress in Quantitative Nondestructive Evaluation*, **18**, 1935-1942.